Improved sensitivity in a modified Berkeley Red Sensor of Transmembrane potential

Marisol X. Navarro,[a] Nels C. Gerstner,[a] Soren M. Lipman,[a] Gabby E. Dolgonos,[a] and Evan W. Miller[a,b,c,*]

[a]Department of Chemistry, [b]Department of Molecular & Cell Biology, and [c]Helen Wills Neuroscience Institute, University of California, Berkeley, California, 94720-1460, USA

ABSTRACT: Voltage imaging is an important complement to traditional methods for probing cellular physiology, like electrode-based patch clamp techniques. Unlike the related Ca^{2+} imaging, voltage imaging provides a direct visualization of bioelectricity changes. We have been exploring the use of sulfonated silicon rhodamine dyes (Berkeley Red Sensor of Transmembrane potential, or BeRST) for voltage imaging. In this study, we explore the effect of converting BeRST to diEt BeRST, by replacing the dimethyl aniline of BeRST with a diethyl aniline group. The new VF dye, diEt BeRST, has a voltage sensitivity of 40% ΔF/F per 100 mV, a 33% increase compared to the original BeRST dye, which has a sensitivity of 30% ΔF/F per 100 mV. In neurons, the cellular brightness of diEt BeRST is about 20% as bright as BeRST, which may be due to the lower solubility of diEt BeRST (300 μM) compared to BeRST (800 μM). Despite this lower cellular brightness, diEt BeRST is able to record spontaneous and evoked action potentials from multiple neurons, simultaneously, and in single trials. Far-red excitation and emission profiles enable diEt BeRST to be used alongside existing fluorescent indicators of cellular physiology, like Ca^{2+}-sensitive Oregon Green BAPTA (OGB). In hippocampal neurons, simultaneous voltage and Ca^{2+} imaging reveals neuronal spiking patterns and frequencies that cannot be resolved with traditional Ca^{2+} imaging methods. This study represents a first step towards describing the structural features that define voltage sensitivity and brightness in silicon rhodamine-based BeRST indicators.

Introduction

Voltage imaging is the direct visualization of cellular membrane potential changes using fluorophores. Imaging voltage changes using fluorescence microscopy provides a powerful complement to traditional, but invasive, electrode-based measurements or indirect Ca^{2+} imaging. Recently, a proliferation of small molecule fluorophores,[1-2] genetically encoded voltage indicators (GEVIs),[3-6] and hybrid approaches[7-11] has made voltage imaging accessible to a wider variety of research laboratories. In particular, our lab has focused on the use of photoinduced electron transfer (PeT) based voltage sensitive fluorophores, or VF dyes. Fluorescein and rhodamine-derived version of VF dyes enable voltage imaging across the blue to far-red / near-infrared window of the spectrum. One VF dye, BeRST, which is based on a sulfonated silicon rhodamine, or Berkeley Red fluorophore, has found utility in a number of applications,[12] including stem-cell derived neurons[13] and cardiomyocytes,[14] cardiomyocytes from human patients,[15] monitoring coupling of plasma membrane and mitochondrial potential during ultradian cycles,[16] screens for improved GEVIs,[17] and dendritic cells.[18] BeRST compares favorably to other dyes and GEVIs in terms of speed, sensitivity, and brightness.[19] However, improved sensitivity and brightness of BeRST-type VF dyes would be a boon for voltage imaging in demanding applications.

One approach to improve voltage sensitivity is to alter the electronics of the donor and acceptor components of VF dyes, typically through substitution of the aniline donor. Although the relationship between aniline substitution patterns and the voltage sensitivity of fluorescein-based VF dyes has been investigated,[20-21] this relationship remains largely unexplored in the context of silicon rhodamine, or Berkeley Red based Sensors of Transmembrane potential (BeRST),[22] VF dyes.

Scheme 1. Diethyl BeRST (diEt BeRST) and BeRST 1

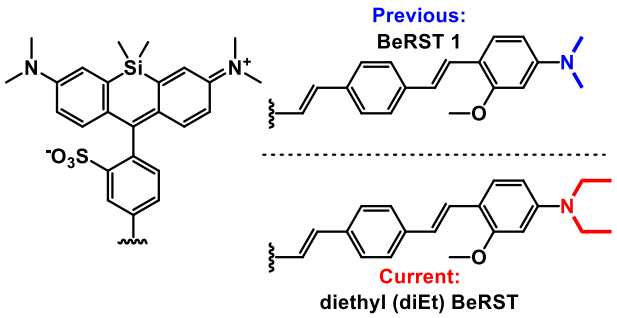

In this study, we asked whether the inclusion of two additional methylene units on the aniline of BeRST would increase the voltage sensitivity of the new dye. Previous studies from our lab showed that increasing the electron richness of the aniline donors improved voltage sensitivity of fluorescein-based VF dyes,[20] but often at the expense of cellular brightness.[21] This subtle change to the original BeRST 1 scaffold – addition of 2 carbon and 4 hydrogen atoms – creates an ethyl-substituted aniline, or diethyl BeRST ("diEt BeRST", **Scheme 1**).

We find that diEt BeRST has improved voltage sensitivity compared to the original BeRST. However, diEt BeRST has lower solubility and has lower cellular brightness in living

Table 1. Properties of silicon rhodamine / Berkeley Red-based voltage-sensitive fluorophores

Dye	λ_{abs} (nm)	λ_{em} (nm)	ε^a ($M^{-1}cm^{-1}$)	$\Phi_f{}^b$	$\varepsilon \times \Phi_{fl}$	Sol.^{c} (mM)	BRT^d	$\Delta F/F^e$	SNR^e	BRT^f	$\Delta F/F^g$	SNR^g
diEt BeRST	658	673	149,000	0.13	19,370	0.3	22%	40% ± 2%	22	40%	13% ± 2%	39
BeRST	658	681	150,000	0.02	3,000	0.8	100%	30% ± 1%	94	100%	10% ± 2%	54

[a]Extinction coefficient measured in TBS buffer with 0.1% SDS, pH7.5. [b]Quantum yield with SiTMR as a standard (0.32).[23] [c]Solubility in DMSO. [d]Brightness in HEK cells with 1 µM dye. [e]Per 100 mV, in voltage-clamped HEK cells. Error is S.E.M, *n* = 7 and *n* = 6 cells for diEt BeRST and BeRST, respectively. [f]Brightness in neurons with 1 µM dye. [g]In stimulated neurons, measuring evoked action potentials. Error is S.E.M, *n* = 16 and *n* = 15 cell trace averages (15 APs averaged per cell) for diEt BeRST and BeRST.

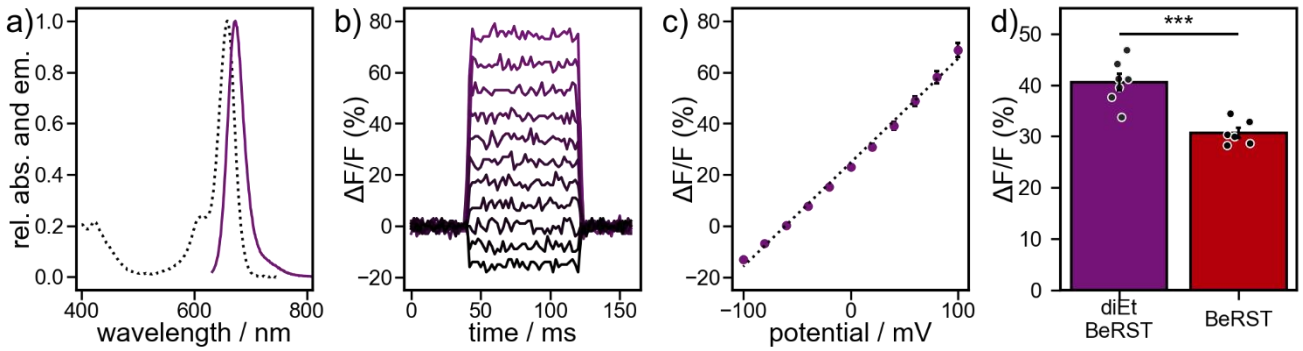

Figure 1. Characterization of diEt BeRST. **a**) Plot of relative absorbance (dotted black line) or emission intensity (solid purple line) for diEt BeRST. Spectra were acquired in pH = 7.5 buffer (50 mM TBS, 150 mM NaCl, 0.1% w/w SDS). **b**) Plot of fractional change in fluorescence (ΔF/F) over time in HEK cells stained with 1 µM of diEt BeRST under voltage clamp conditions. Cells were held at -60 mV and stepped to hyper- or depolarizing potentials (±100 mV) in 20 mV increments. **c**) Plot of %ΔF/F vs final membrane potential for diEt BeRST. Data are the mean ΔF/F. Error bars are S.E.M. for *n* = 7 cells, across 4 different experiments. If error bars are not visible, they are smaller than the marker. Dotted line is the linear fit through the data (R^2 = 0.995). **d**) Plot of mean voltage sensitivity per 100 mV in voltage-clamped HEK cells for diEt BeRST and BeRST. *** p < 0.0002. Circles are the voltage sensitivity for each measured cell, n = 7 (diEt BeRST), n = 6 (BeRST). Error bars are S.E.M.

cells, despite its higher molecular brightness *in vitro*. Despite its decreased cellular brightness, the large voltage sensitivity of diEt BeRST enables high-speed voltage imaging in neurons and multi-color imaging of voltage and Ca^{2+} in the same cells.

Results and Discussion

DiEt BeRST can be synthesized in a single step from previously reported precursor compounds, bromo-Berkeley Red[22] and a phenylenevinylene subunit[24] derived from diethylaminosalicylaldehyde (**Scheme S1**). A Pd-catalyzed Heck coupling using Pd_2dba_3 and QPhos[25] provides diEt BeRST under relatively mild reaction conditions compared to the previously reported BeRST synthesis.[22]

DiEt BeRST retains the photophysical characteristics of silicon-rhodamines, with a maximum absorbance at 658 nm and maximum emission at 673 nm, extinction coefficient of 149,000 $M^{-1}cm^{-1}$, and fluorescence quantum yield (Φ_f) of 0.13 (**Figure 1a, Table 1)**. DiEt BeRST localizes to the plasma membrane of HEK293T cells (**Figure 2a,b**). DiEt BeRST is voltage-sensitive, with a ΔF/F of 40% ± 2% per 100 mV (*n* = 7 cells, S.E.M.) in voltage-clamped HEK293T cells (**Figure 1b,c, Table 1**). This is significantly higher than the voltage-sensitivity of BeRST, which is 30% ± 1% per 100 mV (*n* = 6 cells, S.E.M; p = 0.0004, two-tailed t-test, **Figure 1d**, **Table 1**).

In HEK293T cells, diEt BeRST is dimmer than BeRST, when loaded and imaged under identical conditions (**Figure 2a-c**, **Table 1**). The cellular brightness of diEt BeRST, or the fluorescence intensity from diEt BeRST when loaded in cells, is about 4.5× lower than BeRST (**Figure 2c**, **Table 1**).

Since the molecular brightness of diEt BeRST is about 6× larger than BeRST in an *in vitro* context (**Table 1**), we hypothesize the decrease in cellular brightness is because of the lower membrane loading efficiency of diEt BeRST, likely related to its lower water solubility. The solubility of diEt BeRST is ~300 µM while BeRST is approximately 800 µM (**Table 1**).

We previously observed a similar juxtaposition of molecular and cellular brightness for lipophilic, fluorescein-based VF dyes.[21] The VF dye iPrVF has an additional 2 carbons on the aniline donor compared to VF2.1.Cl and possesses a higher Φ_f (0.28 vs 0.12). However, iPrVF has an overall lower cellular brightness (1.0 vs 3.4).

Additional evidence supporting the low solubility hypothesis is that the use of the non-ionic surfactant, Pluronic F-127 improves the cellular brightness of diEt BeRST by approximately three-fold (**Figure S1a**). However, the use of Pluronic F-127 ("F-127") with BeRST does not increase cellular brightness. Even with the use of F-127, the cellular brightness is less than BeRST. Given this observation and

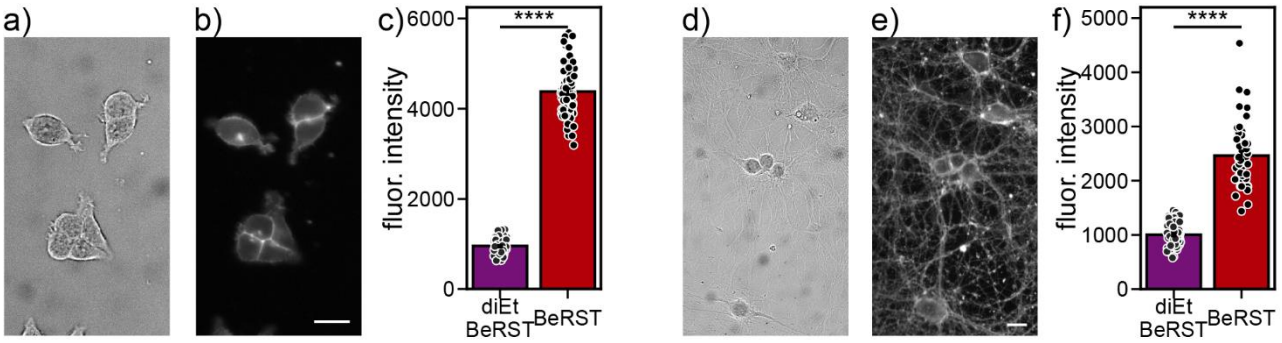

Figure 2. Fluorescence imaging of diEt BeRST in HEK 293T cells and rat hippocampal neurons. **a**) Transmitted light and **b**) wide field epifluorescence image of HEK293T cells stained with diEt BeRST (1 µM). Scale bar is 20 µm. **c**) Plot of fluorescence intensity of either diEt BeRST or BeRST staining in HEK293T cells. **d**) Transmitted light and **e**) wide field epifluorescence image of rat hippocampal neurons stained with diEt BeRST (1 µM). Scale bar is 20 µm. **f**) Plot of fluorescence intensity of either diEt BeRST or BeRST staining in neurons. Bars are the mean value. Error bars are standard error of the mean (S.E.M.) for n = 73 (diEt BeRST, HEK293T), 69 (diEt BeRST, neurons), 67 (BeRST, HEK293T), or 49 (BeRST, neurons) cells. Each point represents the fluorescence intensity for a single cell. **** indicates a p-value of <0.0001 (two-tailed t-test).

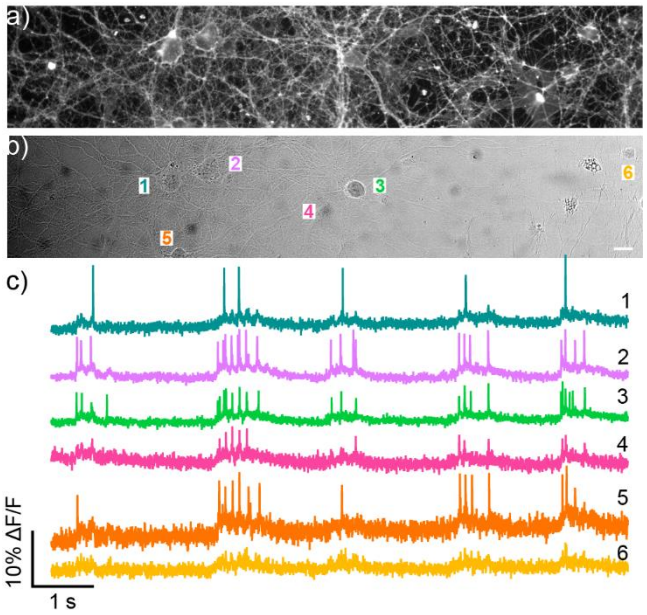

Figure 3. Optical recordings of spontaneous neuronal activity in rat hippocampal neurons using diEt BeRST. **a**) Widefield epifluorescence and **b**) transmitted light image of rat hippocampal neurons stained with 1 µM diEt BeRST. **c**) Plots of ΔF/F vs time for the indicated neurons in panels a/b. Optical recordings are acquired at 500 Hz. Scale bar is 20 µm.

the potential adverse effects of F-127 on cellular physiology,[26] we opted to forego the use of F-127 for subsequent characterization of diEt BeRST. Other loading methods, for example, pre-complexation with bovine serum albumin (BSA) also boost the fluorescence intensity of diEt BeRST, have little effect on BeRST, and may be more well-tolerated by cells (**Figure S1b**). We find that the pre-complexation of diEt BeRST with BSA prior to loading improves the cellular brightness to about 40% of the level of BeRST (**Figure S1b**).

Because of the limited solubility and decreased brightness of diEt BeRST, SNR is compromised in both HEK cells and neurons (**Figure S3c,f**, **Table 1**). The SNR of diEt BeRST in whole cell patch clamped HEK cells is about 23% of the SNR of BeRST in the same conditions (**Table 1, Figure S3c,f**). The photostability of diEt BeRST is marginally better than BeRST (**Figure S2**).

DiEt BeRST stains primary rat hippocampal neurons (**Figure 2d,e**). In neurons, the cellular brightness of diEt BeRST is lower than BeRST (**Figure 2f, Table 1**). DiEt BeRST is about 2.5× dimmer than BeRST in neurons, which is not as large as the difference in brightness in HEK293T cells (4.5× lower). One explanation for the different performance in neurons compared to HEK293T cells is the larger membrane surface area of neurons (>60,000 μm^2)[27] compared to HEK cells (~2,000 μm^2)[28] provides greater lipophilic surfaces for the poorly-soluble diEt BeRST.

In neurons, diEt BeRST can detect spontaneously-firing action potentials across multiple cells with a time resolution of 2 ms (**Figure 3**). DiEt BeRST shows good sensitivity to neuronal action potentials, or rapid changes in membrane potential, with a ΔF/F of 13% (± 2%, standard error of the mean, S.E.M., n = 16 cells) compared to a ΔF/F of 10% for BeRST (± 2%, S.E.M., n = 15 cells, **Table 1**, **Figure S3e**). These differences were not statistically significant (p = 0.10, two-tailed t-test). Unlike HEK293T cells, where a dramatic difference exists in the signal-to-noise-ratio (SNR) for a 100 mV step (**Figure S3f**, **Table 1**), in neurons, the SNR for an action potential is only slightly lower – a direct consequence of the improved cellular brightness of diEt BeRST in neurons relative to HEK293T cells.

The photostability of diEt BeRST neurons appears similar to that of BeRST when making repeated measurements of evoked APs **(Figure S4**). The shape of APs recorded by diEt BeRST, as measured by the full width at half-maximal (FWHM) for each AP remains beneath 150% of its original value after 10 repeated trials (**Figure S4d**). On the other hand, the FWHM of APs recorded with BeRST are ~550% of their original value (**Figure S4d**). The average ΔF/F of APs recorded with BeRST drops to 50% of its original value after 10 trials, with diEt BeRST is unchanged (**Figure S4b**). The photostability of both dyes in neurons is similar (**Figure S4c**).

The far-red to NIR spectra of diEt BeRST allows cells to be co-stained with other fluorescent indicators for multi-color functional imaging (**Figure 4a-d**). Neurons stained

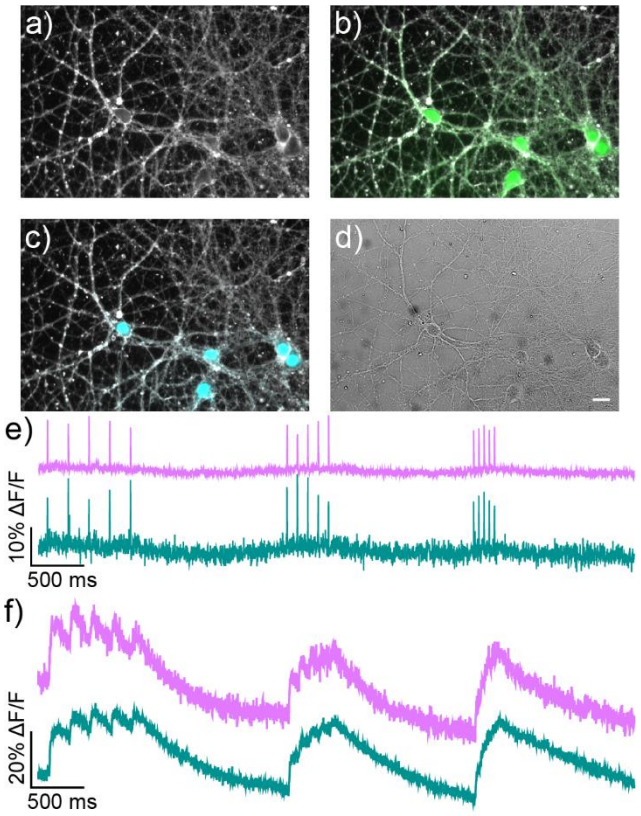

Figure 4. Multi-color imaging in rat hippocampal neurons with diEt BeRST. Neurons were stained with diEt BeRST, Oregon Green BAPTA (OGB), and Hoechst 33342 (1 µM for all dyes). Widefield epifluorescence **a**) diEt BeRST, **b**) diEt BeRST (grey) and OGB (green), **c**) diEt BeRST (grey) and Hoechst (cyan), and **d)** transmitted light image of rat hippocampal neurons. Scale bar is 20 µm. Plots of ΔF/F vs time for **e)** diEt BeRST or **f)** OGB. Colors indicate the same neuron, observed first under voltage imaging and then under Ca^{2+} imaging.

simultaneously with diEt BeRST (**Figure 4a**), Oregon Green BAPTA (OGB, **Figure 4b**), and Hoechst 33342 (**Figure 4c**) enabled interrogation of membrane potential and cytosolic Ca^{2+} fluctuations with nuclear localization.

We evoked action potentials in neurons using a stimulating electrode, as before, and recorded the membrane potential changes using diEt BeRST. We then repeated the stimulation and recorded the Ca^{2+} transients using OGB. APs were induced at frequencies of 5, 10, and 20 Hz. When imaged consecutively, both diEt BeRST and OGB report increases in intensity when the field stimulation was applied, revealing changes in both membrane potential and intracellular calcium, respectively (**Figure 4e,f**).

OGB resolves individual action potentials at 5 Hz, but when action potentials were delivered at 10 and 20 Hz, it becomes hard to distinguish the individual APs (**Figure 4f**). On the other hand, diEt BeRST is able to resolve individual APs from field stimulation at 5, 10, and 20 Hz (**Figure 4e**), highlighting caution in the over interpretation of Ca^{2+} indicator data for determining the number or frequency of underlying action potentials, since linear combinations in the number or frequency of APs could give similar changes in Ca^{2+} imaging fluorescence outputs. Our data reveal that this is a problem even for synthetic indicators, like OGB, which possess fast binding/unbinding kinetics compared to genetically encoded Ca^{2+} indicators.[29]

Conclusion

A small structural change to the far-red voltage-sensitive fluorophore BeRST yields diEt BeRST, which shows improved voltage sensitivity over the parent indicator. However, the decreased solubility and lower cellular brightness decreases the overall performance of diEt BeRST in living cells. Despite the reduced SNR in HEK293T cells and neurons compared to the parent BeRST dye, the improved sensitivity of diEt BeRST enables single-trial recordings of action potentials in neurons (**Figure 3)** and resolution of fast spiking that cannot be resolved by Ca^{2+} imaging (**Figure 4**).

We find that even a small change – addition of two methylene units – can profoundly alter the sensitivity and cellular accumulation of BeRST-based dyes. This study represents a first step towards describing the structural features that define voltage sensitivity and brightness in silicon rhodamine-based BeRST indicators. Future work will be directed towards improving the solubility and membrane accumulation of BeRST derivatives in addition to improving voltage sensitivity.

ASSOCIATED CONTENT

Supporting Information. Synthetic methods, experimental details, and supporting figures. This material is available free of charge via the Internet.

AUTHOR INFORMATION

Corresponding Author

* evanwmiller@berkeley.edu

ACKNOWLEDGMENT

Research reported here is supported by the National Institute of General Medical Sciences and Neurological Disorders and Stroke of the National Institutes of Health under award numbers F32GM139263 (N.C.G.), T32GM066698 (M.X.N. and G.E.D.), and R01NS098088 (E.W.M.). S.M.L. was supported by a Graduate Research Fellowship from the National Science Foundation (NSF-GRFP). E.W.M. acknowledges support from the LGR Innovation Awards program. We thank Drs. Hasan Celik, Raynald Giovine, and Pines Magnetic Resonance Center's Core NMR Facility (PMRC Core) for spectroscopic assistance. The instruments used in this work were supported by the PMRC Core as well as by NIH S10OD024998.

REFERENCES

1. Liu, P.; Miller, E. W., Electrophysiology, Unplugged: Imaging Membrane Potential with Fluorescent Indicators. *Accounts of Chemical Research* **2020,** *53* (1), 11-19.

2. Yan, P.; Acker, C. D.; Biasci, V.; Judge, G.; Monroe, A.; Sacconi, L.; Loew, L. M., Near-infrared voltage-sensitive dyes based on chromene donor. *Proceedings of the National Academy of Sciences* **2023,** *120* (34), e2305093120.

3. Hochbaum, D. R.; Zhao, Y.; Farhi, S. L.; Klapoetke, N.; Werley, C. A.; Kapoor, V.; Zou, P.; Kralj, J. M.; Maclaurin, D.; Smedemark-Margulies, N.; Saulnier, J. L.; Boulting, G. L.; Straub, C.; Cho, Y. K.; Melkonian, M.; Wong, G. K.; Harrison, D. J.; Murthy, V. N.; Sabatini, B. L.; Boyden, E. S.; Campbell, R. E.; Cohen, A. E., All-optical electrophysiology in mammalian neurons using engineered microbial rhodopsins. *Nat Methods* **2014,** *11* (8), 825-33.

4. Lin, M. Z.; Schnitzer, M. J., Genetically encoded indicators of neuronal activity. *Nature Neuroscience* **2016,** *19* (9), 1142-1153.

5. Kannan, M.; Vasan, G.; Haziza, S.; Huang, C.; Chrapkiewicz, R.; Luo, J.; Cardin, J. A.; Schnitzer, M. J.; Pieribone, V. A., Dual-polarity voltage imaging of the concurrent dynamics of multiple neuron types. *Science (New York, N.Y.)* **2022,** *378* (6619), eabm8797.

6. Evans, S. W.; Shi, D. Q.; Chavarha, M.; Plitt, M. H.; Taxidis, J.; Madruga, B.; Fan, J. L.; Hwang, F. J.; van Keulen, S. C.; Suomivuori, C. M.; Pang, M. M.; Su, S.; Lee, S.; Hao, Y. A.; Zhang, G.; Jiang, D.; Pradhan, L.; Roth, R. H.; Liu, Y.; Dorian, C. C.; Reese, A. L.; Negrean, A.; Losonczy, A.; Makinson, C. D.; Wang, S.; Clandinin, T. R.; Dror, R. O.; Ding, J. B.; Ji, N.; Golshani, P.; Giocomo, L. M.; Bi, G. Q.; Lin, M. Z., A positively tuned voltage indicator for extended electrical recordings in the brain. *Nat Methods* **2023,** *20* (7), 1104-1113.

7. Grenier, V.; Daws, B. R.; Liu, P.; Miller, E. W., Spying on Neuronal Membrane Potential with Genetically Targetable Voltage Indicators. *Journal of the American Chemical Society* **2019,** *141* (3), 1349-1358.

8. Sundukova, M.; Prifti, E.; Bucci, A.; Kirillova, K.; Serrao, J.; Reymond, L.; Umebayashi, M.; Hovius, R.; Riezman, H.; Johnsson, K.; Heppenstall, P. A., A Chemogenetic Approach for the Optical Monitoring of Voltage in Neurons. *Angewandte Chemie (International ed. in English)* **2019,** *58* (8), 2341-2344.

9. Abdelfattah, A. S.; Kawashima, T.; Singh, A.; Novak, O.; Liu, H.; Shuai, Y.; Huang, Y.-C.; Campagnola, L.; Seeman, S. C.; Yu, J.; Zheng, J.; Grimm, J. B.; Patel, R.; Friedrich, J.; Mensh, B. D.; Paninski, L.; Macklin, J. J.; Murphy, G. J.; Podgorski, K.; Lin, B.-J.; Chen, T.-W.; Turner, G. C.; Liu, Z.; Koyama, M.; Svoboda, K.; Ahrens, M. B.; Lavis, L. D.; Schreiter, E. R., Bright and photostable chemigenetic indicators for extended in vivo voltage imaging. *Science (New York, N.Y.)* **2019,** *365* (6454), 699-704.

10. Deal, P. E.; Liu, P.; Al-Abdullatif, S. H.; Muller, V. R.; Shamardani, K.; Adesnik, H.; Miller, E. W., Covalently Tethered Rhodamine Voltage Reporters for High Speed Functional Imaging in Brain Tissue. *Journal of the American Chemical Society* **2020,** *142* (1), 614-622.

11. Zhang, Y.; Zhang, D.; Huang, T.; Gillett, A. J.; Liu, Y.; Hu, D.; Cui, L.; Bin, Z.; Li, G.; Wei, J.; Duan, L., Multi-Resonance Deep-Red Emitters with Shallow Potential-Energy Surfaces to Surpass Energy-Gap Law. *Angewandte Chemie International Edition* **2021,** *60* (37), 20498-20503.

12. Walker, A. S.; Raliski, B. K.; Nguyen, D. V.; Zhang, P.; Sanders, K.; Karbasi, K.; Miller, E. W., Imaging Voltage in Complete Neuronal Networks Within Patterned Microislands Reveals Preferential Wiring of Excitatory Hippocampal Neurons. *Frontiers in neuroscience* **2021,** *15*, 643868.

13. Puppo, F.; Sadegh, S.; Trujillo, C. A.; Thunemann, M.; Campbell, E. P.; Vandenberghe, M.; Shan, X.; Akkouh, I. A.; Miller, E. W.; Bloodgood, B. L.; Silva, G. A.; Dale, A. M.; Einevoll, G. T.; Djurovic, S.; Andreassen, O. A.; Muotri, A. R.; Devor, A., All-Optical Electrophysiology in hiPSC-Derived Neurons With Synthetic Voltage Sensors. *Frontiers in cellular neuroscience* **2021,** *15*, 671549.

14. Huebsch, N.; Charrez, B.; Neiman, G.; Siemons, B.; Boggess, S. C.; Wall, S.; Charwat, V.; Jæger, K. H.; Cleres, D.; Telle, Å.; Lee-Montiel, F. T.; Jeffreys, N. C.; Deveshwar, N.; Edwards, A. G.; Serrano, J.; Snuderl, M.; Stahl, A.; Tveito, A.; Miller, E. W.; Healy, K. E., Metabolically driven maturation of human-induced-pluripotent-stem-cell-derived cardiac microtissues on microfluidic chips. *Nature biomedical engineering* **2022,** *6* (4), 372-388.

15. Moreno, J. D.; Bhagavan, D.; Li, A.; Gerstner, N. C.; Miller, E. W.; Huebsch, N.; Cresci, S.; Silva, J. R., Pulsus Alternans in Cardiogenic Shock Recapitulated in Single Cell Fluorescence Imaging of a Patient's Cardiomyocyte. *Circulation. Heart failure* **2022,** *15* (2), e008855.

16. Yang, S.; Yamazaki, S.; Cox, K. H.; Huang, Y.-L.; Miller, E. W.; Takahashi, J. S., Coupling-dependent metabolic ultradian rhythms in confluent cells. *Proceedings of the National Academy of Sciences* **2022,** *119* (45), e2211142119.

17. Tian, H.; Davis, H. C.; Wong-Campos, J. D.; Park, P.; Fan, L. Z.; Gmeiner, B.; Begum, S.; Werley, C. A.; Borja, G. B.; Upadhyay, H.; Shah, H.; Jacques, J.; Qi, Y.; Parot, V.; Deisseroth, K.; Cohen, A. E., Video-based pooled screening yields improved far-red genetically encoded voltage indicators. *Nature Methods* **2023,** *20* (7), 1082-1094.

18. Hanč, P.; Gonzalez, R. J.; Mazo, I. B.; Wang, Y.; Lambert, T.; Ortiz, G.; Miller, E. W.; von Andrian, U. H., Multimodal control of dendritic cell functions by nociceptors. *Science (New York, N.Y.)* **2023,** *379* (6639), eabm5658.

19. Milosevic, M. M.; Jang, J.; McKimm, E. J.; Zhu, M. H.; Antic, S. D., In Vitro Testing of Voltage Indicators: Archon1, ArcLightD, ASAP1, ASAP2s, ASAP3b, Bongwoori-Pos6, BeRST1, FlicR1, and Chi-VSFP-Butterfly. *eNeuro* **2020,** *7* (5).

20. Woodford, C. R.; Frady, E. P.; Smith, R. S.; Morey, B.; Canzi, G.; Palida, S. F.; Araneda, R. C.; Kristan, W. B., Jr.; Kubiak, C. P.; Miller, E. W.; Tsien, R. Y., Improved PeT molecules for optically sensing voltage in neurons. *Journal of the American Chemical Society* **2015,** *137* (5), 1817-24.

21. Boggess, S. C.; Lazzari-Dean, J. R.; Raliski, B. K.; Mun, D. M.; Li, A. Y.; Turnbull, J. L.; Miller, E. W., Fluorescence lifetime predicts performance of voltage sensitive fluorophores in cardiomyocytes and neurons. *RSC chemical biology* **2021,** *2* (1), 248-258.

22. Huang, Y. L.; Walker, A. S.; Miller, E. W., A Photostable Silicon Rhodamine Platform for Optical Voltage Sensing. *Journal of the American Chemical Society* **2015,** *137* (33), 10767-76.

23. Zhou, X.; Fang, Y.; Wimalasiri, V.; Stains, C. I.; Miller, E. W., A long-wavelength xanthene dye for photoacoustic imaging. *Chemical communications (Cambridge, England)* **2022,** *58* (85), 11941-11944.

24. Deal, P. E.; Kulkarni, R. U.; Al-Abdullatif, S. H.; Miller, E. W., Isomerically Pure Tetramethylrhodamine Voltage Reporters. *Journal of the American Chemical Society* **2016,** *138* (29), 9085-8.

25. Stambuli, J. P.; Stauffer, S. R.; Shaughnessy, K. H.; Hartwig, J. F., Screening of homogeneous catalysts by fluorescence resonance energy transfer. Identification of catalysts for room-temperature Heck reactions. *Journal of the American Chemical Society* **2001,** *123* (11), 2677-8.

26. Sutachan, J.-J.; Montoya, J. V.; Xu, F.; Chen, D.; Blanck, T. J. J.; Recio-Pinto, E., Pluronic F-127 affects the regulation of cytoplasmic Ca2+ in neuronal cells. *Brain Research* **2006,** *1068* (1), 131-137.

27. Dai, J.; Sheetz, M. P.; Wan, X.; Morris, C. E., Membrane tension in swelling and shrinking molluscan neurons. *The Journal of neuroscience : the official journal of the Society for Neuroscience* **1998,** *18* (17), 6681-92.

28. Bandmann, V.; Mirsanaye, A. S.; Schäfer, J.; Thiel, G.; Holstein, T.; Mikosch-Wersching, M., Membrane capacitance recordings resolve dynamics and complexity of receptor-mediated endocytosis in Wnt signalling. *Scientific Reports* **2019,** *9* (1), 12999.

29. Chen, T. W.; Wardill, T. J.; Sun, Y.; Pulver, S. R.; Renninger, S. L.; Baohan, A.; Schreiter, E. R.; Kerr, R. A.; Orger, M. B.; Jayaraman, V.; Looger, L. L.; Svoboda, K.; Kim, D. S., Ultrasensitive fluorescent proteins for imaging neuronal activity. *Nature* **2013,** *499* (7458), 295-300.

Table of Contents artwork: